



## Research Article

# Multifunctional Amine Mesoporous Silica Spheres Modified with Multiple Amine as Carriers for Drug Release

Yan Li,<sup>1</sup> Fangxiang Song ,<sup>2</sup> Yu Guo,<sup>2</sup> Liang Cheng,<sup>3</sup> and Qianlin Chen <sup>1</sup>

<sup>1</sup>Institute of Advanced Technology, Guizhou University, Guiyang 550025, China

<sup>2</sup>School of Chemistry and Chemical Engineering, Guizhou University, Guiyang 550025, China

<sup>3</sup>School of Electrical Engineering, Guizhou University, Guiyang 550025, China

Correspondence should be addressed to Qianlin Chen; [qlchen@gzu.edu.cn](mailto:qlchen@gzu.edu.cn)

Received 27 April 2017; Accepted 18 July 2017; Published 8 January 2018

Academic Editor: Yan Zou

Copyright © 2018 Yan Li et al. This is an open access article distributed under the Creative Commons Attribution License, which permits unrestricted use, distribution, and reproduction in any medium, provided the original work is properly cited.

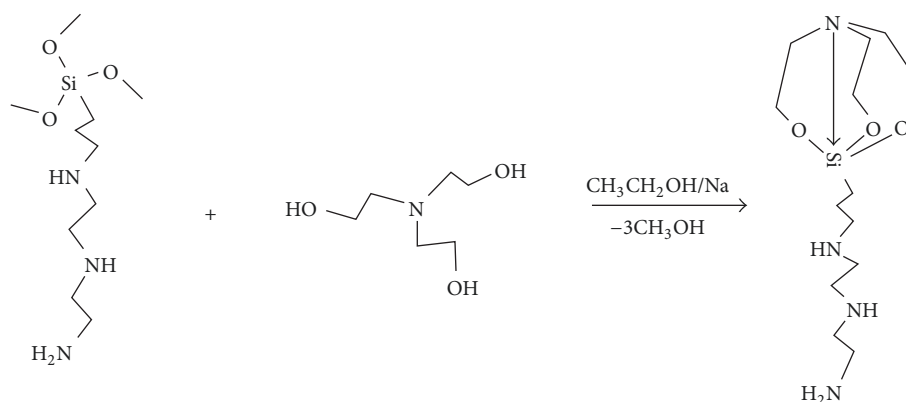
Mesoporous silica spheres were synthesized by using Stöber theory (MSN-40). Calcination of the mesostructured phase resulted in the starting solid. Organic modification with aminopropyl groups resulted in two MSN-40 materials: named MSN-NH<sub>2</sub> and MSN-DQ-40, respectively. These two kinds of samples with different pore sizes (obtained from 3-[2-(2-aminoethylamino)ethylamino]propyl-trimethoxy-silane (NQ-62) and modified NQ-62) showed control of the delivery rate of ibuprofen (IBU) from the siliceous matrix. The obtained sample from modified NQ-62 has an increased loading rate and shows better control of the delivery rate of IBU than the obtained sample from NQ-62. These three solids were characterized using standard solid state procedures. During tests of in vitro drug release, an interesting phenomenon was observed: at high pH (pH 7.45), IBU in all carriers was released slowly; at low pH (pH 4.5), only a part of the IBU was slowly released from this carrier within 25 hours; most IBU was effectively confined in mesoporous material, but the remaining IBU was released rapidly and completely after 25 hours.

## 1. Introduction

Mobil Oil [1] reported M41S mesoporous silica materials in 1992. In 2001, Vallet-Regi et al. used MCM-41 as a drug carrier of ibuprofen [2] creating the field of mesoporous silica biomedical research. Although there are many kinds of inorganic nanomaterials that have been widely reported for biomedical applications [3], mesoporous silica nanoparticles (MSNs) show their unique features in this field. MSNs can withstand thermal and mechanical stress as well as pH and oxidative degradation. They have low toxicity and good biocompatibility [4–7]. The drug loading capacity can be changed by adjusting the pore diameter. Surface modification can control the drug release rate [8]. These nanoparticles have the following remarkable characteristics [8–12]: (1) there exist ordered pore networks, uniform pore size, and precise control of drug loading and release; (2) the large pore volume can store more drugs; (3) high surface area means that the adsorption ability of drug is strong; (4) the surface contains a large amount

of Si-OH—functional group functionalization offers better control of drug loading and releasing. These unique features have made mesoporous materials an excellent material for drug delivery and many other potential applications [13, 14].

This process requires the loading and release of high quantities of drugs due to their special mesoporous structure characteristics [15, 16]. This loading can utilize organic functional groups [17–21] on the surface of the mesoporous materials. Mesoporous silica has many Si-OH surface groups that can be functionalized via silane coupling agents [22]: amino, thiol, and cyano. These functional groups offer good adsorption of drugs such as aspirin [23, 24] and ibuprofen [25], but their load capacity is not high and requires a longer time [23, 24, 26, 27]. Casasús et al. [28] used a polyamine chain of silane coupling agents on the surface of mesoporous silica. The polyamine chain was the “door” of material. At low pH, the “door” is opened. At neutral or basic conditions, the door was closed. Gao et al. [26] concluded that this improves drug loading and offers pH-sensitive release.



SCHEME 1: Synthesis rout of MDNQ.

There are two approaches to making an ibuprofen delivery nanoparticle via Stöber theory [29]: (1) using the grafting method processes modification for mesoporous silica with NQ-62 [(3-[2-(2-amino-ethyl amino)ethylamino]propyl-trimethoxysilane)] as modifying agent or (2) MDNQ ( $\gamma$ -N-[(arylideneaminoethyl)-aminoethyl]aminopropyl-2,8,9-trioxa-5-aza-1-sila-bicyclo[3, 3, 3]undecanes) could be obtained by modifying NQ-62, via grafting to load IBU. Here, we highlight the NQ-62, MDNQ-modified mesoporous silica in loading and releasing of IBU. Routes (1) and (2) release IBU at pH 7.45. There is slow release at pH 4.5. Release is slow over the first 25 hours but becomes quicker after 25 hours.

## 2. Experimental Section

**Reagents.** Tetraethyl orthosilicane (TEOS, AR, TianJin, China), cetyltrimethylammonium bromide (CTAB, AR, TianJin), ammonia solution ( $\text{NH}_3 \cdot \text{H}_2\text{O}$ , AR, ChenDu, China), triethanolamine ( $\text{N}(\text{CH}_2\text{CH}_2\text{OH})_3$ , AR, TianJin, China), 3-[2-(2-aminoethylamino)ethylamino]propyl-trimethoxysilane (NQ-62, 95%, ShangHai, China), methanol (MeOH, AR, TianJin, China), phosphate buffer saline (PBS, pH 7.45 and pH 4.5), and ibuprofen (IBU, GC) were purchased from Aladdin (Shanghai China) and used without any further purification. All water was deionized water.

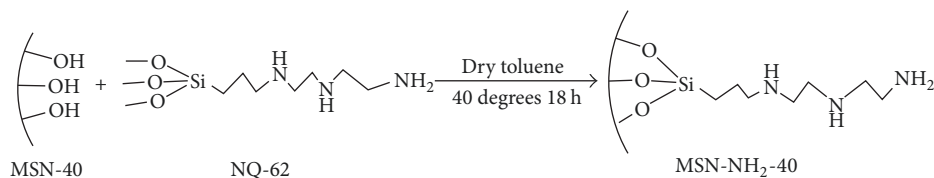
**Instrumentation.** The powder X-ray diffraction (XRD) patterns were recorded on a Bruker D8 X-ray diffractometer with Ni-filtered  $\text{CuK}\alpha$  radiation (40 kv, 40 mA). Fourier-transform infrared (FI-IR) spectra were collected on Nicolet iS50 spectrophotometer using KBr pellets, and nitrogen sorption isotherms were measured at with a Micromeritics ASAP 2020. Before measurements, the samples were degassed in a vacuum at  $100^\circ\text{C}$  for at least 12 hours. The Brunauer-Emmett-Teller (BET) method was utilized to calculate the specific surface areas ( $S_{\text{BET}}$ ) using adsorption data. By using the Barrett-Joyner-Halenda (BJH) model, the pore volumes and pore size distributions were derived from the adsorption branches of isotherms. Transmission electron microscopy (TEM) of samples was observed on JEM-2100 electron microscopy at 160 KV. Scanning electron microscopy (SEM) images were

taken with a JEOL-JSM-7500F electron microscope operating at 20 KV. Thermogravimetric analysis (TG-DTA/DSC) was conducted in air on a STA 449C Jupiter® thermal analyzer. The samples were heated from 30 to  $1000^\circ\text{C}$  with a heating rate of  $10^\circ\text{C}/\text{min}$  in air.

**2.1. Synthesis of Mesoporous Silica.** To 220 ml of deionized water mixed with 80 ml of methanol, there was added ammonia water to a pH of 11.24. Next, 0.58 g of CTAB was added with uniform mixing with a rotating speed of 1200 rpm. The temperature rose to  $40^\circ\text{C}$ . Then 5 ml of TEOS was added dropwise. After 1 min, a white precipitate appeared. The reaction proceeded for 3 hours and was then aged for 3 hours. It was filtered to obtain a white solid. The solid was dried at  $70^\circ\text{C}$  in air for 24 hours. This was then calcined at  $420^\circ\text{C}$ . The material was named MSN-40.

**2.2. Modification of NQ-62.** We used polyamine silane coupling agents [25, 30, 31]. To a 50 ml round-bottom flask, 15 ml absolute ethanol was added with 0.1g of sodium. This was stirred to dissolve the sodium. Then, 10.3 g of NQ-62 (0.1 equivalent) was added and mixed with 5 g (0.1 equivalent) of triethanolamine. This was stirred to reflux for 10 hours, cooled, and rotary evaporated to remove the absolute ethanol. The solution obtained at  $175^\circ\text{C}$  was heated at high temperature with stirring for 36 hours to yield a red brown, sticky substance. We added a small amount of ether to wash the triethanolamine and then added acetone to remove the NQ-62. Anhydrous ethanol solution was added to the precipitate. This was filtered and vacuum distilled to yield a brown viscous material named MDNQ. The experimental process is as mentioned in Scheme 1.

**2.3. Functionalization of Mesoporous Silica.** For functionalization, a 2010 report on the multiamine functionalization of mesoporous silica was used [26]. Here, 400 mg MSN-40 was dispersed in 50 ml dry toluene followed by 1.6 ml NQ-62 and 18 hours of stirring at  $40^\circ\text{C}$ . This was filtered while hot and washed three times with dry toluene to remove unreacted NQ-62. The solid obtained at  $70^\circ\text{C}$  was dried in an oven for 24 hours. The substance was named the MSN-NH<sub>2</sub>-40 (Scheme 2): an aminofunctional mesoporous silica.



SCHEME 2: NQ-62 modified mesoporous silica MSN-40.

The 1.6 g of MDNQ was dissolved in 40 ml aqueous solution, and 400 mg of MSNs was dispersed in solution at 50°C with 1.5 hours' reaction. This was filtered hot and washed three times with deionized water to remove excess MDNQ. The solid was obtained at 65°C after 24 hours of air drying. The substance was named as MSN-DQ-40.

#### 2.4. Loading of IBU

**2.4.1. Loading of IBU.** The 198 mg of IBU was dissolved in 30 ml (6.6 mg/ml). This was treated with 200 mg of MSN-40, MSN-NH<sub>2</sub>-40, or MSN-DQ-40. The solution was stirred for 36 hours or 72 hours at room temperature with a stirring speed of 500 rpm. The nanoparticles were collected with a 4000 rpm centrifuge for 30 min. The solid was dried at 50°C in air dry oven for 24 hours. To measure IBU loading, 2 ml of the supernatant fluid was diluted to 50 ml and measured at 264 nm on a UV-6100s. This was repeated in triplicate taking the average. The IBU loading quantity was obtained via the following formula [21, 32]:

$$\text{wt\%} = \frac{(m_1 - (50/2) CV)}{(m_2 + (m_1 - (50/2) CV))}. \quad (1)$$

$m_1$  is showing the initial mass of IBU;  $m_2$  is showing mesoporous adsorbent added to hexane solution;  $C$  is showing IBU concentration of the solution prepared by diluting 2 ml of filtrates to 50 ml in volumetric flask;  $V$  is showing the volume of hexane solution for drug loading.

**2.4.2. Releasing of IBU.** In our release experiment, each sample is loaded in phosphate buffered saline (PBS) at pH 4.5 and pH 7.45. The nanoparticles (60 mg) were placed in 8000–14000 MWCO dialysis bags with 8 ml PBS. The dialysis solution was 250 ml of PBS at pH 4.5 or pH 7.45 at 37°C. The stirring speed was 500 rpm. Three mL aliquots were taken periodically and measured with absorbance as described above [32, 33]. At the same time, equal volume of fresh release fluid was added. Calculation of the accumulated concentration of released IBU is based on the following equation:

$$C_c = C_t + \frac{v}{V} \sum_0^{t-1} C_t. \quad (2)$$

$C_c$  is the real concentration of IBU released at time  $t$ ;  $C_t$  is the apparent concentration measured by UV-vis spectrometry of the release fluid sample at time  $t$ ;  $v$  is the volume of sample taken at the predetermined time intervals;  $V$  is the total volume of release fluid.

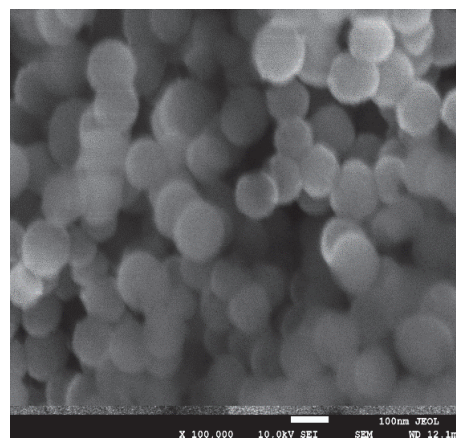


FIGURE 1: MSN-40 of scanning electron microscope.

### 3. Results and Discussion

**3.1. Characteristics of Sample.** Figure 1 is the MSN-40 of the scanning electron microscope. The materials are spherical with an average particle size of  $100 \pm 17$  nm. Figure 2 shows TEM images of the three samples at different magnifications. These samples show agglomeration, nonuniformity, and spherical morphologies. Spherical MSN-40 porous structure offers uniform distribution of multiamine chains [21] inside and outside the pores. The open-framework structure becomes increasingly vague in Figures 2(d), 2(e), and 2(f) indicating that multiamine chain is grafted inside and outside the pores.

Figure 3 shows MSN-40, MSN-NH<sub>2</sub>-40, MSN-DQ-40, MSN-NH<sub>2</sub>-40/IBU, and MSN-DQ-40/IBU adsorption/desorption isotherms as well as the distribution of pore size and pore volume. Figure 3(a) shows five samples with typical type IV adsorption isotherms indicating the presence of a mesoporous channel. Samples MSN-DQ-40/IBU and MSN-NH<sub>2</sub>-40 and MSN-NH<sub>2</sub>-40/IBU are characteristic with H<sub>3</sub> type IV material whose hysteresis loop indicates that the materials have no obvious saturated adsorption platform. The pore structure is not uniform reflecting a tablet slit structure or fracture structure [32]. However, the MSN-DQ-40 and MSN-40 are type IV materials with an H<sub>1</sub> hysteresis loop characteristic. The MSN-40 has linear absorption at low pressure suggesting that the test material is mesoporous; the relative pressure at  $0.2 < p/p_0 < 0.28$  shows rapid increase. The relative pressure at  $0.3 < p/p_0 < 0.8$  shows no obvious hysteresis loop—the material is partially hollow. Uniformity

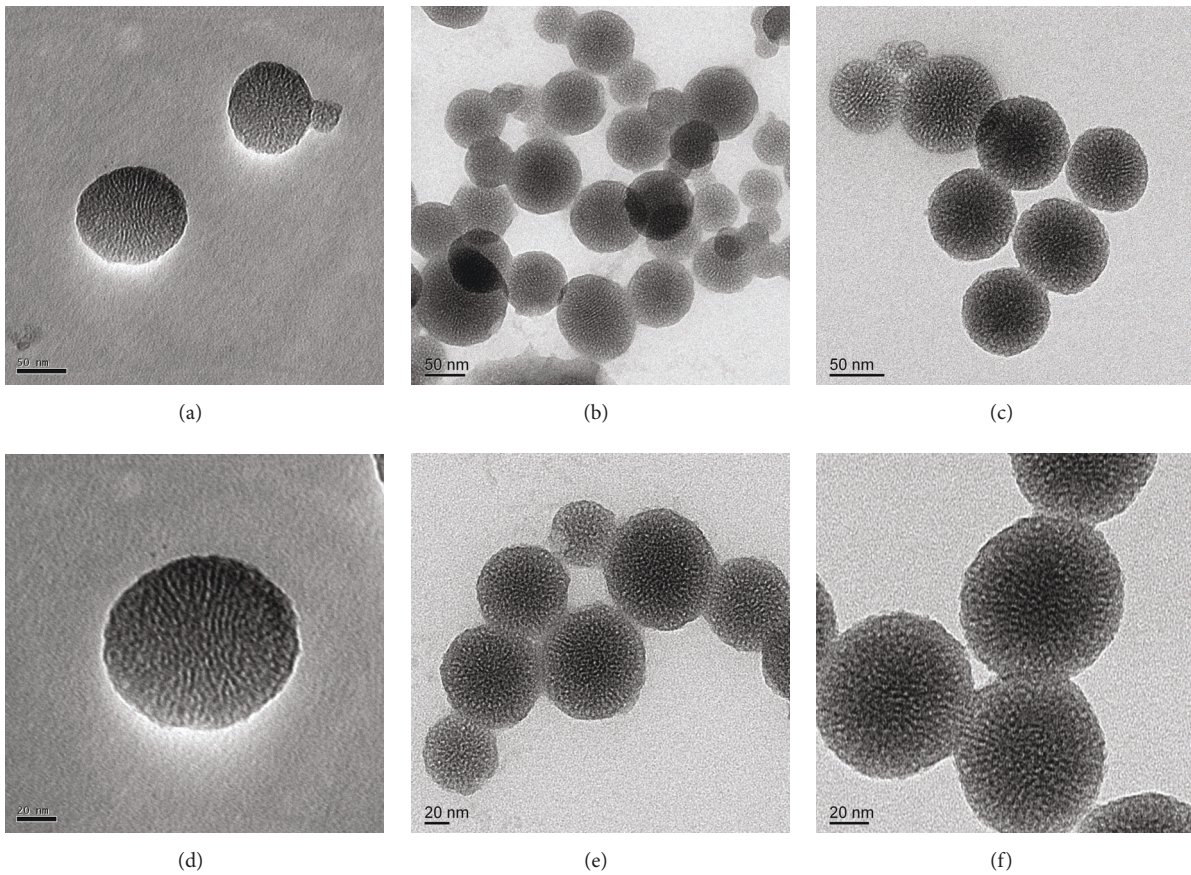


FIGURE 2: Under 50 nm and 20 nm size of the transmission electron microscopy (TEM) picture: MSN-40 (a, d), MSN-NH<sub>2</sub>-40 (b, e), and MSN-DQ-40 (c, f).

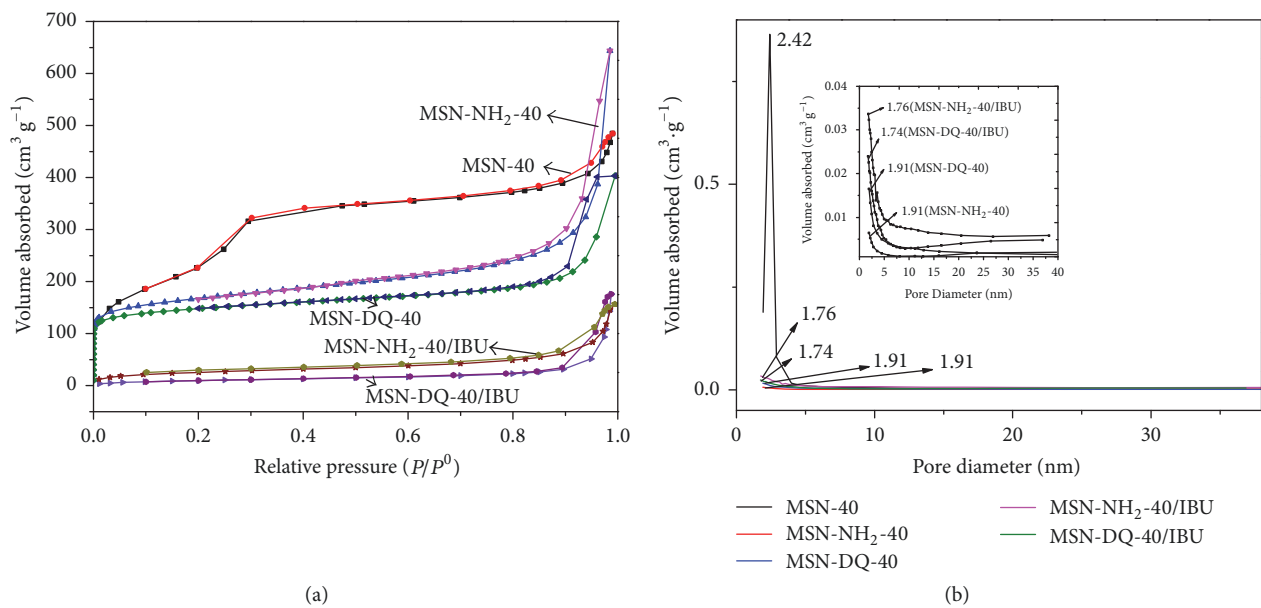
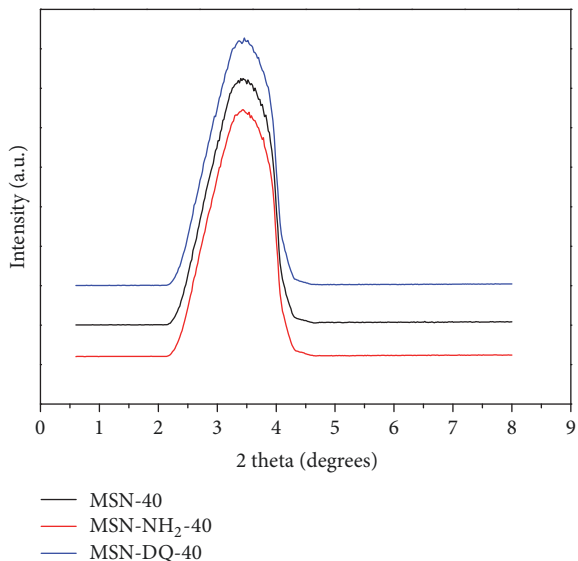


FIGURE 3: Nitrogen adsorption/desorption isotherms (a) and pore size distributions of samples (b): MSN-40, MSN-NH<sub>2</sub>-40, MSN-DQ-40, MSN-NH<sub>2</sub>-40/IBU, and MSN-DQ-40/IBU.

TABLE 1: Parameters of samples: MSN-40, MSN-NH<sub>2</sub>-40, and MSN-DQ-40.

Sample	Specific surface area ( $S_{\text{BET}}$ ) ( $\text{m}^2\text{g}^{-1}$ )	Pore volume ( $V_p$ ) ( $\text{cm}^3\text{g}^{-1}$ )	BJH adsorption pore diameter (nm)
MSN-40	987.79	0.75	2.42
MSN-NH <sub>2</sub> -40	569.58	0.033	1.91
MSN-DQ-40	508.75	0.096	1.91
MSN-NH <sub>2</sub> -40/IBU	90.41	0.006	1.76
MSN-DQ-40/IBU	37.014	0.016	1.74

FIGURE 4: XRD patterns of samples: MSN-40, MSN-NH<sub>2</sub>-40, and MSN-DQ-40.

is very good. At  $0.8 < p/p_0 < 1$  area, the material has a hysteresis loop due to the clearance hole, that is, the mesoporous structure of the cavity or the accumulation of clearance particles or mesoporous structure of the cavity. The corresponding pore size distribution plots were calculated with the BJH method [34] (Figure 3(b)). The MSN-40, MSN-NH<sub>2</sub>-40, MSN-DQ-40, MSN-NH<sub>2</sub>-40, and MSN-DQ-40 have average pore diameters of 2.42 nm, 1.91 nm, 1.91 nm, 1.76 nm, and 1.74 nm. This confirms amine functionalization and loading of IBU. The average pore volume and surface area were estimated via the BET method (see Table 1). Table 1 shows that, after modification, the MSN-40's pore size, specific surface area, and pore volume decrease. The decreases of specific surface areas are due to the reason that the presence of pendant organic chains covalently bonded to the inorganic network have the ability to partially block the entrance of nitrogen molecules [35], and indicated that organic groups were fastened inside mesopores. After IBU loading, their texture parameters also decrease indicating multiamine chains into mesoporous channels.

The XRD of patterns of MSN-40, MSN-NH<sub>2</sub>-40 and MSN-DQ-40 are shown in Figure 4. An obvious peak (100) can be observed for all these samples indicating that they are

ordered mesoporous structures [9, 36, 37]. After modification with amino groups, the intensity of peaks (100) of MSN-40, MSN-NH<sub>2</sub>-40, and MSN-DQ-40 changed. The position shifted from  $3.44^\circ$  (MSN-40) to  $3.42^\circ$  (MSN-NH<sub>2</sub>-40) and  $3.46^\circ$  (MSN-DQ-80) indicating that amine groups have been implanted into mesoporous channels of MSN-40 [25, 28, 30].

Figures 5(a) and 5(b) are the infrared spectrum of ibuprofen and MDNQ, respectively. Figure 5(a) of marked peak is MDNQ characteristic peak [25, 30, 31], IR (Nujolmull,  $\text{cm}^{-1}$ ): 3383s ( $\nu_{\text{as}}\text{NH}$ ), 2973vs ( $\nu_{\text{as}}\text{CH}_2$ ), 2865vs ( $\nu_{\text{s}}\text{CH}_2\text{O}$ ), 2843s ( $\nu_{\text{s}}\text{CH}_2\text{N}$ ), 1653m ( $\delta\text{NH}_2$ ), 1576m ( $\delta\text{CH}_2\text{N}$ ), 1472s ( $\delta_{\text{s}}\text{CH}_2\text{O}$ ), 1416m ( $\omega\text{CH}_2\text{N}$ ), 1314 ( $\omega\text{CH}_2\text{O}$ ), 1121vs ( $\nu\text{C-O}$ ), 1016s ( $\nu\text{C-O}$ ), 1054s ( $\nu_{\text{as}}\text{NC}_3$ ), 1035s ( $\nu_{\text{as}}\text{NC}_3$ ), 940s ( $\nu\text{C-C}$ ), 911s ( $\nu_{\text{s}}\text{NC}_3$ ), 888 $\omega$  ( $\nu\text{C-N}$ ), 812m ( $\nu_{\text{as}}\text{Si-O}$ ), 780vs ( $\nu_{\text{as}}\text{Si-O}$ ), 760vs ( $\nu_{\text{as}}\text{Si-O}$ ), 725s ( $\nu_{\text{s}}\text{Si-O}$ ), 685 $\omega$  ( $\nu_{\text{s}}\text{Si-O}$ ), and 585m ( $\nu\text{Si-N}$ ). The Si-O bond exhibits peaks at  $459\text{ cm}^{-1}$  (Figure 5(b)). The  $2843\text{ cm}^{-1}$  and  $2939\text{ cm}^{-1}$  bands are stretching vibration peaks of  $-\text{CH}_2$  of NQ-62 and  $3350\text{ cm}^{-1}$  and  $3284\text{ cm}^{-1}$  are the NH stretching vibration peaks of the primary and secondary amines in NQ-62,  $1066\text{ cm}^{-1}$  is the stretching vibration peak of C-N, and the shear vibration peak at  $1471\text{ cm}^{-1}$  is  $-\text{CH}_2$ .

Figures 5(c) and 5(d) are the infrared spectra of MSN-40 loaded with IBU and sample MSN-NH<sub>2</sub>-40 and MSN-DQ-40 loading IBU, respectively. Figure 5(c) contains secondary amine and primary amine N-H stretching vibration peak ( $3500\text{--}3000\text{ cm}^{-1}$ ). The stretching vibration peaks of Si-O-Si appear at  $1078\text{ cm}^{-1}$  and  $1230\text{ cm}^{-1}$ , and the asymmetry vibration peaks appear at  $807\text{ cm}^{-1}$ ; Si-OH has a symmetrical stretching vibration peak at  $954\text{ cm}^{-1}$ , but Figure 5(d) does not show this peak. This is because the head group on the NQ-62 interacted with the Si-OH of the hydrogen bond. The stretching vibration peaks of the Si-O bond appear at  $459\text{ cm}^{-1}$ . Figure 5(c) has peaks at  $2810\text{ cm}^{-1}$  and  $2930\text{ cm}^{-1}$  from the  $-\text{CH}_2$  of stretching vibration peak. There are almost no peaks at  $2810\text{ cm}^{-1}$  and  $2930\text{ cm}^{-1}$  in Figures 5(c) and 5(d) indicating that the templating agent is almost removed. The bands at  $2843\text{ cm}^{-1}$  and  $2937\text{ cm}^{-1}$  appear in Figures 5(a) and 5(b) and are the stretching vibration peaks of  $-\text{CH}_2$  in NQ-62 and MDNQ. The single peak at  $2853\text{ cm}^{-1}$  in Figures 5(b), 5(c), and 5(d) is the stretching vibration peak of NH in primary amine because of the presence of tertiary amines in MDNQ with no free N-H absorption peak. The alkyl group peaks at  $2864\text{ cm}^{-1}$  and  $2967\text{ cm}^{-1}$  of the IBU could be clearly observed. The characteristic absorption peaks of  $-\text{COOH}$  at  $1725\text{ cm}^{-1}$  and benzene ring of absorption peaks at

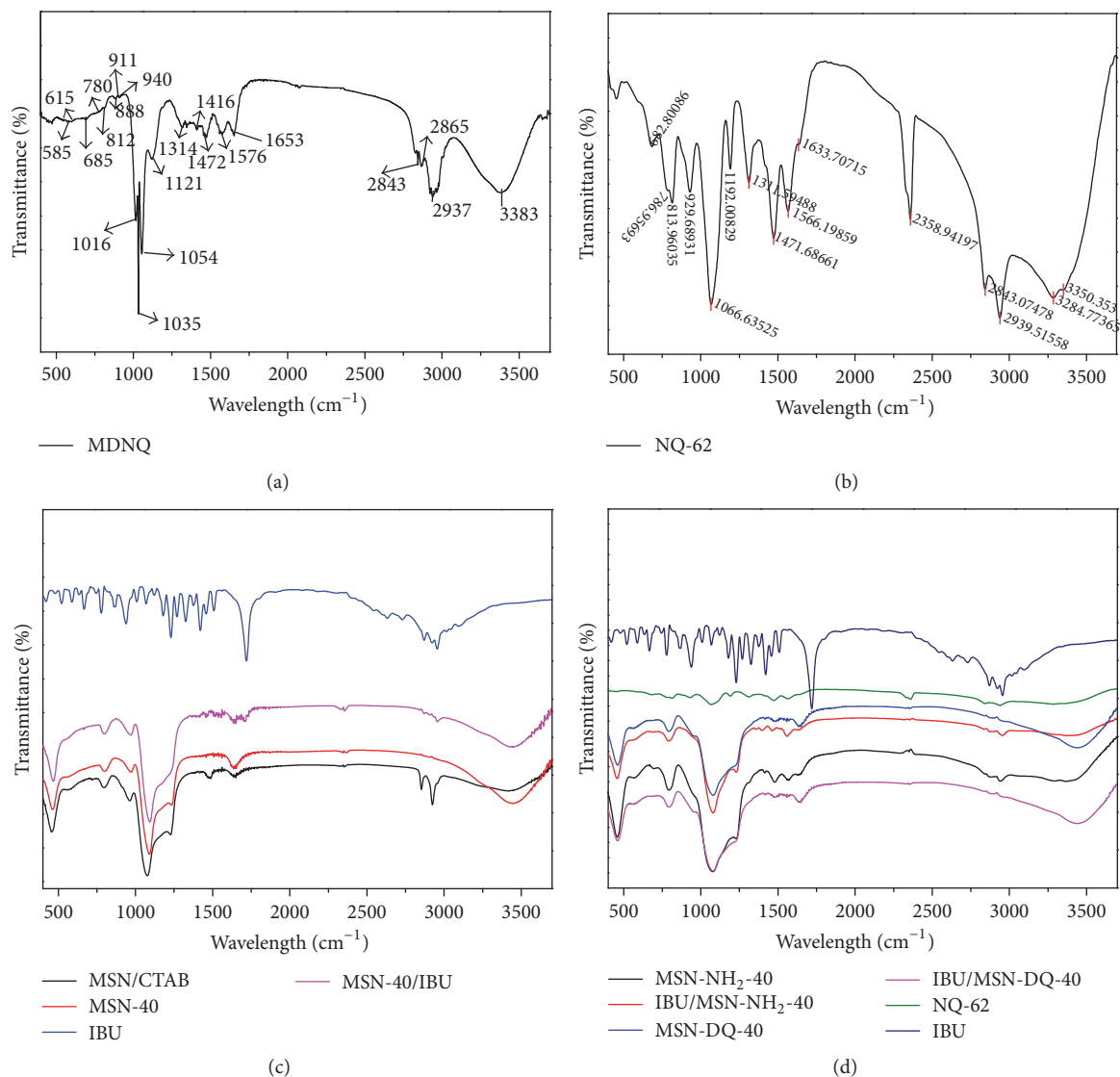


FIGURE 5: FTIR spectra of sample: MDNQ (a), NQ-62 (b), MSN-40/MSN-40/IBU (c), and IBU/MSN-NH<sub>2</sub>-40/IBU/MSN-DQ-40 (d).

1430–1600  $\text{cm}^{-1}$  of IBU are obvious. The -COOH peak of the MSN/IBU system decreased significantly, and a new peak at 1569  $\text{cm}^{-1}$  is obvious because of the coexistence of interaction between -COOH and -NH<sub>2</sub> forming a -CO-NH. We conclude that the IBU has been successfully loaded on the surface of the mesoporous silica, that NQ-62 is successfully grafted on the surface of the mesoporous silica, that the MDNQ is successfully grafted on the surface of MSN, and that the template agent is almost completely removed.

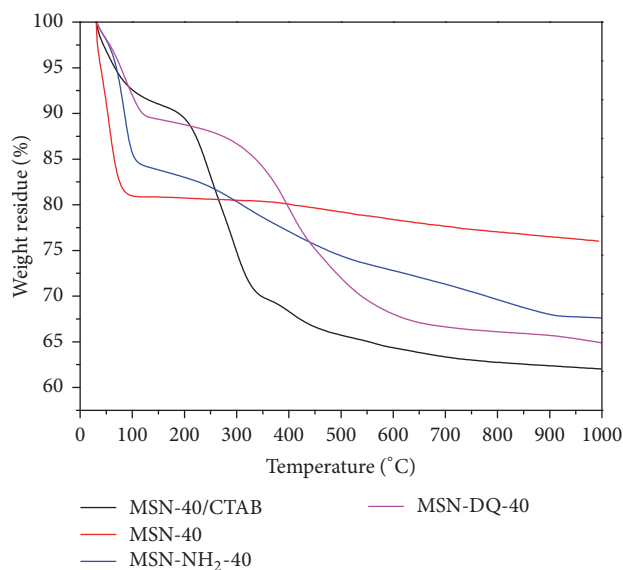
Figure 6 shows the TG curves of the materials. All samples show an obvious weight loss up to 100°C due to the desorption of physically adsorbed water [38]. In addition, there is no obvious weight loss attributed to the disintegration of MSN-40 suggesting that the MSN-40 is thermally stable. The MSN-40/CTAB has significant weight loss due to surfactant CTAB loss of MSN-40/CTAB at 100–500°C. For amine functionalized samples, the TG curves have a rapid weight

loss at 200–800°C, which is due to the removal of multiamine groups [21]. This is significant evidence of the existence of amine groups on the surface and inner pore of MSN-40 [21, 38, 39]. The MSN-DQ-40 can be further confirmed due to fairly obvious weight loss compared to MSN-NH<sub>2</sub>-40. This indicates that the grafting amount of multiamine groups on MSN-DQ-40 is much higher than MSN-NH<sub>2</sub>-40.

**3.2. Loading and Releasing of IBU.** Table 2 shows the loading rate of MSN-40, MSN-NH<sub>2</sub>-40, and MSN-DQ-40 at 36 hours and 72 hours. Within 36 hours, the MSN-NH<sub>2</sub>-40 loading rate of IBU was only 10.68%, while MSN-DQ-40 reached 49.47%. Within 72 hours, the MSN-NH<sub>2</sub>-40 reached 46.93% for IBU suggesting that the loading rate of NQ-62 after modification is low. The pore diameter and volume as well as the specific surface area are reduced, which decreases adsorption. The MDNQ-modified MSN has an increased

TABLE 2: IBU-loaded amount of sample: MSN-40, MSN-NH<sub>2</sub>-40, and MSN-DQ-40.

Sample	Loading (%) 36 h	Loading (%) 72 h
MSN-40		48.07
MSN-NH <sub>2</sub> -40	10.68	46.93
MSN-DQ-40	49.47	

FIGURE 6: TG curves of sample: MSN-40/CTAB (black line), MSN-40 (red line), MSN-NH<sub>2</sub>-40 (blue line), and MSN-DQ-40 (pink line).

loading rate. The loading time is shorter because the MDNQ quickly enriches IBU to improve the loading rate.

Figures 7(a), 7(b), 7(c), and 7(d) are MSN-40, MSN-NH<sub>2</sub>-40, and MSN-DQ-40 at pH 7.45 and pH 4.5 buffer solution for cumulative release, respectively. Figure 7(a) shows that it is complete within 50 hours. The buffer solution (pH 7.45) MSN-40 can slowly release IBU at pH 4.5. The IBU release rate is only 19% showing that acidic conditions inhibit IBU release. Figures 7(b) and 7(c) are at pH 7.45. The MSN-NH<sub>2</sub>-40 and MSN-DQ-40 have slow IBU release, and the accumulative release rates are 27% and 30.5%, respectively, at pH 4.5. Within 25 hours, the release is slow after a burst release. This might be because -COOH and -NH<sub>2</sub> form a peptide bond. The amide has slow hydrolysis in the acidic environment with heating (37°C). This is the opposite of the literature [4] reporting a “switch effect” [17–21] in amino-modified mesoporous silica. We achieved an open channel amino-modified mesoporous silica. For Figure 7(d), our experimental condition was that we got the nanoparticles (12 mg) process release of experiment. Figure 7(d) represents the MSN-NH<sub>2</sub>-40 and MSN-DQ-40 in the buffer solution at pH 4.5 release rate of IBU within 26 hours. The MSN-NH<sub>2</sub>-40 slowly releases IBU, and MSN-DQ-40 can release IBU in full. MDNQ offers good enrichment effects for IBU with stable release in a weak acid environment for 24 hours.

## 4. Conclusions

We demonstrated the feasibility of controlling the delivery rate of drugs occluded in MSN-40 matrixes by functionalizing the pore wall with a silane coupling agent and modified silane coupling agent. For IBU, which contains an acid group, the well-ordered MSN-40 matrixes are functionalized with aminopropyl moieties (namely, MSN-NH<sub>2</sub> and MSN-DQ-40) to decrease delivery. They showed pH-responsive control for drug release. At high pH (pH 7.45), IBU drug loaded in MSN-40 matrixes releases slowly within 50 hours; at low pH (pH 4.5), the IBU was slowly released within 25 hours but was released rapidly and completely after 25 hours.

## Conflicts of Interest

The authors declare that there are no conflicts of interest regarding the publication of this paper.

## Acknowledgments

The authors acknowledge financial support from the high-level innovative talents training project of Guizhou province (QKHPTRC[2016]5658) and the First Graduate Student Scientific Research Fund Projects in Guizhou, China (KYJJ, [2016] 09). They thank LetPub (<http://www.letpub.com/>)

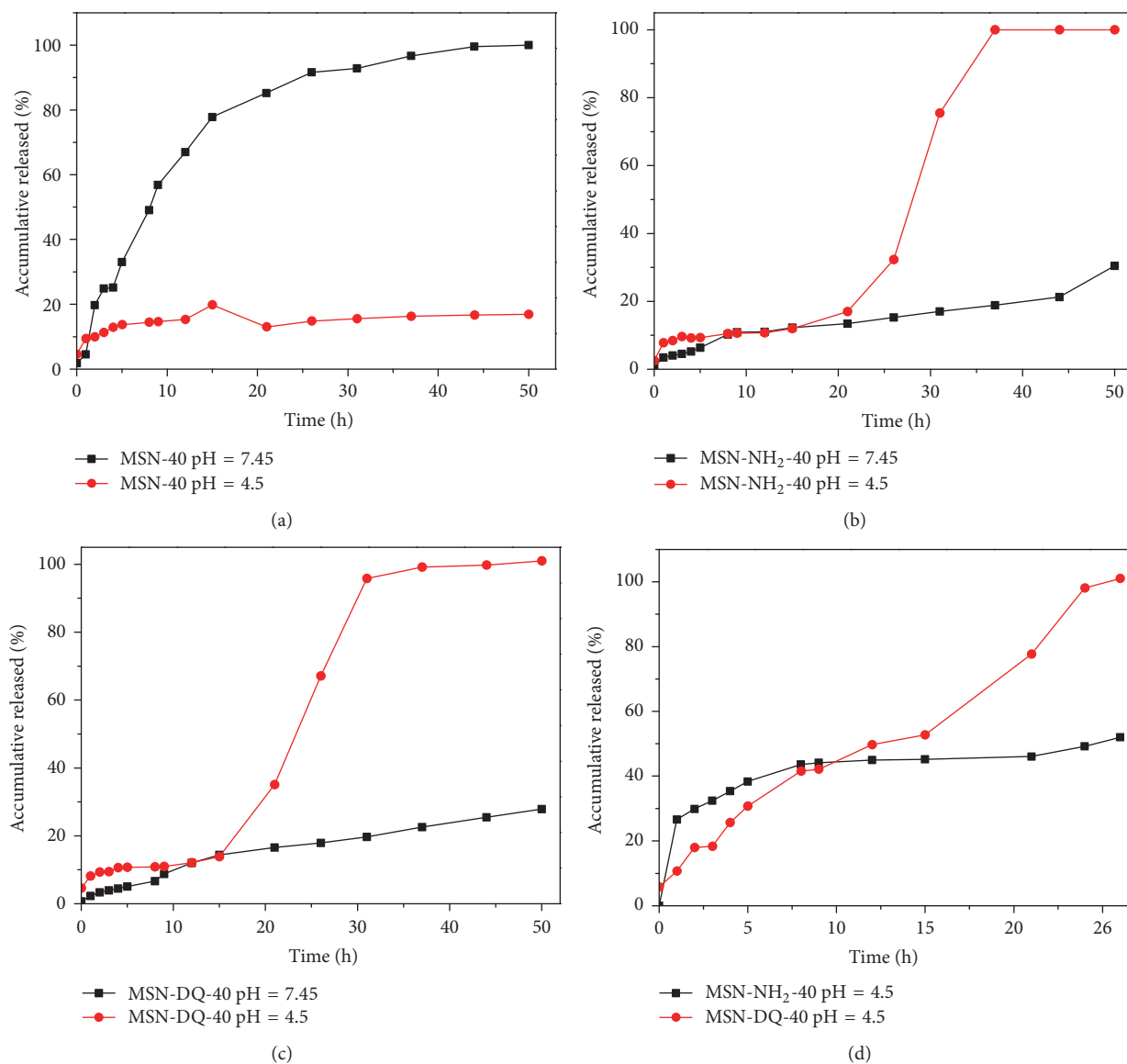


FIGURE 7: IBU releasing of sample: MSN-40/IBU, MSN-NH<sub>2</sub>-40/IBU, and MSN-DQ-40/IBU in pH = 7.45 and pH = 4.5 buffer solution.

for its linguistic assistance during the preparation of this manuscript.

## References

- [1] C. T. Kresge, M. E. Leonowicz, W. J. Roth, J. C. Vartuli, and J. S. Beck, "Ordered mesoporous molecular sieves synthesized by a liquid-crystal template mechanism," *Nature*, vol. 359, no. 6397, pp. 710–712, 1992.
- [2] M. Vallet-Regi, A. Rámila, R. P. Del Real, and J. Pérez-Pariente, "A new property of MCM-41: Drug delivery system," *Chemistry of Materials*, vol. 13, no. 2, pp. 308–311, 2001.
- [3] Z. Hou, C. Li, P. Ma et al., "Up-conversion luminescent and porous NaYF<sub>4</sub>:Yb<sup>3+</sup>, Er<sup>3+</sup>@SiO<sub>2</sub> nanocomposite fibers for anti-cancer drug delivery and cell imaging," *Advanced Functional Materials*, vol. 22, no. 13, pp. 2713–2722, 2012.
- [4] M. J. Mulvihill, B. L. Rupert, R. He, A. Hochbaum, J. Arnold, and P. Yang, "Synthesis of bifunctional polymer nanotubes from silicon nanowire templates via atom transfer radical polymerization," *Journal of the American Chemical Society*, vol. 127, no. 46, pp. 16040–16041, 2005.
- [5] Q. He, J. Shi, F. Chen, M. Zhu, and L. Zhang, "An anticancer drug delivery system based on surfactant-templated mesoporous silica nanoparticles," *Biomaterials*, vol. 31, no. 12, pp. 3335–3346, 2010.
- [6] Q. He, J. Zhang, J. Shi et al., "The effect of PEGylation of mesoporous silica nanoparticles on nonspecific binding of serum proteins and cellular responses," *Biomaterials*, vol. 31, no. 6, pp. 1085–1092, 2010.
- [7] M. Zhu, H. Wang, J. Liu et al., "A mesoporous silica nanoparticulate/ $\beta$ -TCP/BG composite drug delivery system for osteoarticular tuberculosis therapy," *Biomaterials*, vol. 32, no. 7, pp. 1986–1995, 2010.



- [8] Q. He, Y. Gao, L. Zhang et al., "A pH-responsive mesoporous silica nanoparticles-based multi-drug delivery system for overcoming multi-drug resistance," *Biomaterials*, vol. 32, no. 30, pp. 7711–7720, 2011.
- [9] C. Wu, Z. Wang, Z. Zhi, T. Jiang, J. Zhang, and S. Wang, "Development of biodegradable porous starch foam for improving oral delivery of poorly water soluble drugs," *International Journal of Pharmaceutics*, vol. 403, no. 1-2, pp. 162–169, 2011.
- [10] F. Qu, G. Zhu, S. Huang, S. Li, and S. Qiu, "Effective controlled release of captopril by silylation of mesoporous MCM-41," *ChemPhysChem*, vol. 7, no. 2, pp. 400–406, 2006.
- [11] Y. Yang, Y. Jia, L. Gao et al., "Fabrication of autofluorescent protein coated mesoporous silica nanoparticles for biological application," *Chemical Communications*, vol. 47, no. 44, pp. 12167–12169, 2011.
- [12] K. C.-W. Wu and Y. Yamauchi, "Controlling physical features of mesoporous silica nanoparticles (MSNs) for emerging applications," *Journal of Materials Chemistry*, vol. 22, no. 4, pp. 1251–1256, 2012.
- [13] J. Trebosc, J. W. Wiench, S. Huh, V. S.-Y. Lin, and M. Pruski, "Studies of organically functionalized mesoporous silicas using heteronuclear solid-state correlation NMR spectroscopy under fast magic angle spinning," *Journal of the American Chemical Society*, vol. 127, no. 20, pp. 7587–7593, 2005.
- [14] M. Shokouhimehr, Y. Piao, J. Kim, Y. Jang, and T. Hyeon, "A magnetically recyclable nanocomposite catalyst for olefin epoxidation," *Angewandte Chemie International Edition*, vol. 46, no. 37, pp. 7039–7043, 2007.
- [15] C. Urata, H. Yamada, R. Wakabayashi et al., "Aqueous colloidal mesoporous nanoparticles with ethylene-bridged silsesquioxane frameworks," *Journal of the American Chemical Society*, vol. 133, no. 21, pp. 8102–8105, 2011.
- [16] S. Wang, "Ordered mesoporous materials for drug delivery," *Microporous and Mesoporous Materials*, vol. 117, no. 1-2, pp. 1–9, 2009.
- [17] E. Aznar, R. Martínez-Máñez, and F. Sancenón, "Controlled release using mesoporous materials containing gate-like scaffoldings," *Expert Opinion on Drug Delivery*, vol. 6, no. 6, pp. 643–655, 2009.
- [18] E. Aznar, C. Coll, M. Dolores Marcos et al., "Borate-driven gate-like scaffolding using mesoporous materials functionalised with saccharides," *Chemistry - A European Journal*, vol. 15, no. 28, pp. 6877–6888, 2009.
- [19] I. I. Slowing, J. L. Vivero-Escoto, C. W. Wu, and V. S. Y. Lin, "Mesoporous silica nanoparticles as controlled release drug delivery and gene transfection carriers," *Advanced Drug Delivery Reviews*, vol. 60, no. 11, pp. 1278–1288, 2008.
- [20] N. K. Mal, M. Fujiwara, and Y. Tanaka, "Photocontrolled reversible release of guest molecules from coumarin-modified mesoporous silica," *Nature*, vol. 421, no. 6921, pp. 350–353, 2003.
- [21] N. K. Mal, M. Fujiwara, Y. Tanaka, T. Taguchi, and M. Matsukata, "Photo-switched storage and release of guest molecules in the pore void of coumarin-modified MCM-41," *Chemistry of Materials*, vol. 15, no. 17, pp. 3385–3394, 2003.
- [22] M. Vallet-Regí, F. Balas, and D. Arcos, "Mesoporous materials for drug delivery," *Angewandte Chemie*, vol. 46, no. 40, pp. 7548–7558, 2007.
- [23] L. Gao, J. Sun, L. Zhang, J. Wang, and B. Ren, "Influence of different structured channels of mesoporous silicate on the controlled ibuprofen delivery," *Materials Chemistry and Physics*, vol. 135, no. 2-3, pp. 786–797, 2012.
- [24] R. Xing, H. Lin, P. Jiang, and F. Qu, "Biofunctional mesoporous silica nanoparticles for magnetically oriented target and pH-responsive controlled release of ibuprofen," *Colloids and Surfaces A: Physicochemical And Engineering Aspects*, vol. 403, pp. 7–14, 2012.
- [25] S. C. Verma, M. Nasim, and P. S. Venkataramani, "Synthesis and characterization of 3-[2-(2-aminoethylamino)ethylamino]propyl-1-silatrane," *Indian Journal of Chemistry - Section B Organic and Medicinal Chemistry*, vol. 43, no. 8, pp. 1737–1742, 2004.
- [26] Q. Gao, Y. Xu, D. Wu, W. Shen, and F. Deng, "Synthesis, characterization, and in vitro pH-controllable drug release from mesoporous silica spheres with switchable gates," *Langmuir*, vol. 26, no. 22, pp. 17133–17138, 2010.
- [27] P. Botella, A. Corma, and M. Quesada, "Synthesis of ordered mesoporous silica templated with biocompatible surfactants and applications in controlled release of drugs," *Journal of Materials Chemistry*, vol. 22, no. 13, pp. 6394–6401, 2012.
- [28] R. Casásús, M. D. Marcos, R. Martínez-Máñez et al., "Toward the development of ionically controlled nanoscopic molecular gates," *Journal of the American Chemical Society*, vol. 126, no. 28, pp. 8612–8613, 2004.
- [29] W. Stöber, A. Fink, and E. Bohn, "A novel method for synthesis of silica nanoparticles," *Journal of Colloid and Interface Science*, vol. 26, no. 1, pp. 62–69, 1968.
- [30] M. G. Voronkov, V. P. Baryshok, N. F. Lazareva et al., "1-[N-(2-Aminoethyl) aminoalkyl] silatrane and their complexes with CuCl<sub>2</sub>," *Journal of Organometallic Chemistry*, vol. 368, no. 2, pp. 155–161, 1989.
- [31] J.-M. Lin, L. Fang, and W.-T. Huang, "Synthesis of  $\gamma$ -N-[(Arylideneaminoethyl) - Aminoethyl]Aminopropyl-2, 8, 9-Trioxa-6-Aza-1-Sila-Bicyclo [3, 3, 3] Undecanes," *Synthesis and Reactivity in Inorganic, Metal-Organic, and Nano-Metal Chemistry*, vol. 25, no. 9, pp. 1467–1477, 1995.
- [32] Z. S. Eren, S. Tunçer, G. Gezer, L. T. Yildirim, S. Banerjee, and A. Yilmaz, "Improved solubility of celecoxib by inclusion in SBA-15 mesoporous silica: Drug loading in different solvents and release," *Microporous and Mesoporous Materials*, vol. 235, pp. 211–223, 2016.
- [33] L. Gao, J. Sun, L. Zhang, Y. Li, and B. Ren, "Thermal decomposition behavior of amino groups modified bimodal mesoporous silicas as aspirin carrier," *Journal of Nanoscience and Nanotechnology*, vol. 11, no. 12, pp. 10324–10332, 2011.
- [34] C.-J. Tsou, Y. Hung, and C.-Y. Mou, "Hollow mesoporous silica nanoparticles with tunable shell thickness and pore size distribution for application as broad-ranging pH nanosensor," *Microporous and Mesoporous Materials*, vol. 190, pp. 181–188, 2014.
- [35] A. L. P. Silva, K. S. Sousa, A. F. S. Germano et al., "A new organofunctionalized silica containing thioglycolic acid incorporated for divalent cations removal-A thermodynamic cation/basic center interaction," *Colloids and Surfaces A: Physicochemical and Engineering Aspects*, vol. 332, no. 2-3, pp. 144–149, 2009.
- [36] X. Guo, Y. Deng, B. Tu, and D. Zhao, "Facile synthesis of hierarchically mesoporous silica particles with controllable cavity in their surfaces," *Langmuir*, vol. 26, no. 2, pp. 702–708, 2010.
- [37] P. Visuvamithiran, K. Shanthi, M. Palanichamy, and V. Murugesan, "Direct synthesis of Mn-Ti-SBA-15 catalyst for the oxidation of ethylbenzene," *Catalysis Science & Technology*, vol. 3, no. 9, pp. 2340–2348, 2013.

- [38] C. P. Jaroniec, M. Kruk, M. Jaroniec, and A. Sayari, "Tailoring surface and structural properties of MCM-41 silicas by bonding organosilanes," *The Journal of Physical Chemistry B*, vol. 102, no. 28, pp. 5503–5510, 1998.
- [39] M. M. Ayad, N. A. Salahuddin, A. A. El-Nasr, and N. L. Torad, "Amine-functionalized mesoporous silica KIT-6 as a controlled release drug delivery carrier," *Microporous and Mesoporous Materials*, vol. 229, pp. 166–177, 2016.



**Hindawi**  
Submit your manuscripts at  
[www.hindawi.com](http://www.hindawi.com)

